# Analysis and Design of a Special Type Power Transformer Used in Solar Power Plants

Emir Yükselen * ⁂ ‡, Ires Iskender **

* Electrical and Electronics Engineering Department, Gazi University, Ankara, Turkey

⁂ Electrical Design Department, SEM Transformatör Inc., Ankara, Turkey

** Electrical Electronics Engineering Department, Çankaya University, Ankara, Turkey

(emir.yukselen@gazi.edu.tr, ires@cankaya.edu.tr)

‡ Corresponding Author; Emir Yükselen, Electrical and Electronics Engineering Department, Gazi University, Ankara, Turkey, emir.yukselen@gazi.edu.tr,

*Received: 06.03.2022 Accepted: 14.04.2022*

**Abstract-** Due to growing of greenhouse gas emissions and lack of the fossil sources, governments encouraged all scientists and utilities for looking to the alternative energy sources such as solar renewable energy which can help to reduce carbon dioxide emissions. In this respect, Photovoltaic (PV) power plants have become more important in recent years and renewable energy sources integrated into the power system are increasing day by day. Transformers are the main components of electrical grids and are widely used in renewable power plants to transfer the energy they produce to the grid. Accordingly, transformers are one of the most critical equipment of PV plants, and their safe operation and stability in the electrical network are important. This type of transformer is supplied from solar panels through inverters and needs to be customized to work with each system. In this type of transformer, the losses are higher than those for transformers used in electrical power systems supplied by sinusoidal voltage considering existence of different voltage and current harmonics content produced by the inverter. In this study, a special type of PV transformer was designed in accordance with the target performance criteria, taking into account the effects of harmonics, and keeping the transformer losses and temperature rise at a safe level. In this paper also the simulation results are compared with those of experiments test to verify the design procedures.

**Keywords** PV (Photovoltaic); Solar Power Plant (SPP); Transformer; High Frequency (HF) Harmonic; Finite Element Method (FEM)

## 1. Introduction

Due to the inadequacy of fossil fuel resources in recent years, the need for friendly and reliable natural energy sources is one of the most important challenges of our age. As a result, solar photovoltaic power is growing rapidly and plays an important role in power generation. The electrical energy generated by the PV panels is converted into alternating current by the inverter and the alternating current is transferred to the network using a step-up transformer [20-22]. Accordingly, transformers are an important component in the generation and distribution of solar energy. Working conditions and grid integration of solar transformers are very specific. Considering the restrictions on the power and voltage of inverters there are different configurations used in supplying the transformers of Solar Power Plants (SPP). For high power rating applications, more than one inverter can be used to supply the required power.

The power transformer should be designed for specific operating conditions of the SPP, taking into account the harmonic content of the inverters output voltage and current [23, 24]. In some studies, some correction factors such as the k-factor are used in transformer design to take into account the additional losses corresponding to the current harmonic content [1-2]. Some analyses regarding the maximum loading capacity of oil-type transformers used in solar power plants are presented in [3]. Finite element analysis software was also used to simulate the correction factors and validate the calculation of transformer losses in [4-6]. A comparative analysis of design considerations for a solar generation transformer is presented in [7]. In [8], the author evaluates the effect of current harmonics on the k-factor value of the distribution transformer used in different applications and

loading conditions. In [25], magnetic field behaviour analysis of a special type of PV transformer was carried out to investigate the effects of unbalanced operation of inverters on transformer performance. The main criterion for carrying out this work is to approximate the electrical design of a special type of three-phase, three-concentric winding PV transformer with two equal 2.55 MVA low-voltage windings, typically fed by two separate inverters according to the design guide of IEEE C57.159 [11]. The results of HF losses calculated by the method given in IEC 61378-1 [9] are also taken into account. The proposed methodology, incorporated into the production design system using ANSYS Maxwell, enables the assessment of how much the dimensions and quality of the proposed materials for the magnetic core and coils of a transformer are affected by the particular harmonic component of the inverter, so that the manufacturer can guarantee efficiency and stability of the transformer. The main contribution of this study is to establish and validate the design methodology for special type transformers that will operate under certain harmonic content due to the operating conditions of the inverters used in SPP. In this study the effect of the voltage harmonics is not considered because the voltage harmonics do not cause significant increase in core losses of the transformer [10].

## 2. Design Process of the PV Transformer

The design of the transformer to meets their international standard begins with the active part electrical design of the transformer. Afterwards the design of the cooling surface and tank is finished considering transformer losses [14-18].

### *2.1. Specifications*

The electrical design requirements of PV transformer are briefly given in Table 1.

**Table 1.** Transformer requirements

| | |
|---|---|
| Power (MVA) | 5.1 (2.55+2.55) |
| Frequency (Hz) | 60 |
| Cooling system | ONAN |
| Primary voltage (V) | 660-660 |
| Secondary voltage (V) | 34500 |
| Vector group | Dyn11yn11 |
| Off circuit taps on HV | ±5% 2 x 2.5% steps |
| Ambient temperature | 40°C |
| Top oil temperature rise | 60°C |
| Average winding temperature rise | 65°C |
| HV BIL ( Basic Insulation Level) | 170 kV |
| AC test voltage | 70 kV |
| No load loss | Max 3.8 kW |
| Load loss | Max 52 kW |
| Short circuit impedance | 7% ± 10% |

The winding arrangement of the subjected transformer is shown in Figure 1 where high voltage (HV) winding placed radially between two low voltage (LV) windings.

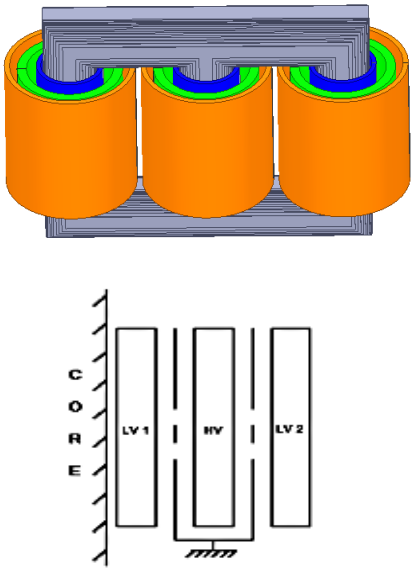


**Fig. 1.** PV transformer winding configuration

### *2.2. Line, Phase Voltages and Currents*

The line and phase to neutral voltages and currents are shown in Table 2.

**Table 2.** Line, phase voltages and currents of the transformer

| Description | LV | HV | | |
|---|---|---|---|---|
| | | Max. | Rated | Min. |
| Line voltage (V) | 660 | 36225 | 34500 | 32775 |
| Phase voltage (V) | 381.1 | 36225 | 34500 | 32775 |
| Line current (A) | 2230.6 | 81.3 | 85.3 | 89.8 |
| Phase current (A) | 2230.6 | 46.9 | 49.3 | 51.9 |

### *2.3. Calculation of Core Section Area, Volt Per Turn, HV and LV Turn Numbers*

The calculation of the initial volt per turn is achieved using the following equation [17].

$$Volt\ /\ Turn = 0.4 \times \sqrt{kVA} = 28.56 \quad (1)$$

The initial LV turns is calculated using equation (2),

$$N = \frac{LV_{LineVolts}}{\sqrt{3} \times Volt\ /\ Turn} = 13.33 \quad (2)$$

The LV turn numbers selected as 13 and consequently, volt per turn will be 29.3. The turn numbers of different HV taps are given in Table 3.

**Table 3.** HV taps and the corresponding turns numbers

| Voltage (kV) | Tap number | Turn numbers |
|---|---|---|
| 32.775 | 1 | 1118 |
| 33.638 | 2 | 1148 |
| 34.500 | 3 | 1177 |
| 35.363 | 4 | 1206 |
| 36.225 | 5 | 1236 |

The core of the subjected transformer is selected as M4 with specification of 0.27 mm thickness and 1.1 w/kg at 1.7 T. In the design procedure, a magnetic flux density of 1.65 T is preferred to keep core losses below the no-load loss value given in Table 1. The core cross-sectional area can be obtained using equation (3). In design procedure the magnetic flux density is preferred as 1.65 T to keep the core losses below the specified no load loss value given in Table 1. The core cross section area can be obtained using equation (3).

$$A = \frac{Volt/Turn}{4.44 \times f \times B} = 0.0667 \tag{3}$$

The diameter of the core is obtained from the following equation considering the core stacking factor of 0.95.

$$d = \sqrt{\frac{4 \times 0.0667}{\pi \times 0.95}} = 0.299 \tag{4}$$

The core diameter for this design is selected as 0.3 m.

*2.4. Winding Design*

A summary of design parameters of windings are presented in Table 4.

**Table 4.** Design parameters of the subjected transformer

| Particulars | $LV_1$ | HV | $LV_2$ |
|---|---|---|---|
| Number of turns per phase | 13 | 1118-1236 | 13 |
| Number of layers | 13 | 19 | 13 |
| Turns per layer | 1 | 66 | 1 |
| Width of conductor, mm | 710 | 9.7 | 710 |
| Thickness of conductor, mm | 1.6 | 2.6 | 1.6 |
| Area of conductor, $mm^2$ | 1136 | 25.22 | 1136 |
| Current density, $A/mm^2$ | 1.96 | 1.95 | 1.96 |
| Inner diameter, mm | 315 | 443 | 649 |
| Interlayer insulation, mm | 0.125 | 0.6 | 0.125 |
| Radial thickness, mm | 31.5 | 86.7 | 31.5 |
| Outer diameter, mm | 377.9 | 617.5 | 714 |
| Winding axial height, mm | 740 | 747 | 740 |

As shown in Table 4, the low voltage windings are the Aluminum foil type and the high voltage winding is the rectangular paper insulated type.

*2.5. Calculation of the Load Loss*

The load losses of the transformer divided into three categories [17],

- Winding and lead connection resistive losses (I2R losses)
- Eddy current loss in the winding
- Stray losses in the tanks and structural parts

The resistive losses at 75 C° are calculated using the following equation;

$$P = K \times j^2 \times W \tag{5}$$

where K is 12.61 for Aluminum, J represents the current density and W is weight of the windings. Hence, resistive losses for windings are calculated as below,

$$P_{LV1} = 12.61 \times 1.96^2 \times 130.7 = 6331$$

$$P_{HV} = 12.61 \times 1.95^2 \times 411 = 19707$$

$$P_{LV2} = 12.61 \times 1.95^2 \times 250 = 12110$$

The eddy losses of each winding can be derived from following equation [13],

$$P_{WE1} = 2I^2 \frac{\rho(MLT)N^2}{h\delta p\eta}\left[\frac{\sinh(2\Delta)+\sin(2\Delta)}{\cosh(2\Delta)-\cos(2\Delta)}\right] + \frac{2}{3}\left(p^2-1\right)\left[\frac{\sinh(\Delta)-\sin(\Delta)}{\cosh(\Delta)+\cos(\Delta)}\right] \tag{6}$$

where, I is the current rms value, N is the winding turns number, p is the total layer of the winding, MLT the mean length of turns, $\Delta$ is the penetration ratio and ρ is the resistivity of conductors.

Using equation (6) the total eddy losses of windings are calculated as 780 W. The losses corresponding to windings connections and the stray losses of structural parts are calculated as 3470 W and 3800 W, respectively.

*2.6. Calculation of the Load Loss with Non-sinusoidal Current*

Additional losses due to current harmonics of the inverter must be precisely estimated and calculated during the design process and overall dimensioning of the transformer. The following methods are given to determine the load loss under certain operating conditions [9, 10].

Total losses under converter operation are calculated by;

$$P_N = I_{LN}^2 \times (R_W + R_C) + (F_{WE} \times P_{WE1}) + F_{CE} \times (P_{CE1} + P_{SE1}) \tag{7}$$

where $I_{LN}$ is the rms value of rated current of converter, $R_W$ is the resistance value of conductors, $R_C$ is the resistance value of connections, $F_{WE}$ is the eddy loss enhancement factor for windings, $P_{WE1}$ is the winding eddy loss with rated current, $F_{CE}$ is the eddy loss enhancement factor for

connections, $P_{CE1}$ is the connection eddy loss with rated current and $P_{SE1}$ is the stray loss of structural parts at rated current. The enhancement factor for connections is obtained from equation (8).

$$F_{CE} = \sum_{1}^{n}\left(\frac{I_h}{I_1}\right)^2 \times h^{0.8} \tag{8}$$

According to references [9, 10], $F_{SE} = F_{CE}$

The enhancement factor for windings eddy loss can be derived from equation (9). The axial and radial stray fluxes can be obtained from finite element method at fundamental frequency.

$$F_{WE} = \frac{P_{WEax1}}{P_{WE1}} \times \sum_{1}^{n}\left(\frac{I_h}{I_1}\right)^2 \times h^2 + \frac{P_{WErad1}}{P_{WE1}} \times \sum_{1}^{n}\left(\frac{I_h}{I_1}\right)^2 \times h^{0.5} \tag{9}$$

The axial ( $P_{WEax1}$ ) and radial ( $P_{WErad1}$ ) eddy losses are calculated as follows [12];

$$P_{WEax1} = \frac{B_a^2 W^2 \sigma t^2}{24} \tag{10}$$

$$P_{WErad1} = \frac{B_r^2 W^2 \sigma l^2}{24} \tag{11}$$

where, $B_a$ is the axial magnetic flux and $B_r$ is the radial magnetic flux obtained from the FEM analyses and is the conductivity parameter. The harmonics considered in this study are given in Table 5. These data are obtained from the output of the PWM-based converters used by the customer. The design methodology presented in this study is a general method and does not depend on which harmonics are dominant.

**Table 5.** Current harmonics

| Number | (Hz) | (%) |
|---|---|---|
| 1 | 60 | 100% |
| 2 | 120 | 0.273 |
| 5 | 300 | 0.170 |
| 7 | 420 | 0.170 |
| 13 | 780 | 0.175 |
| 77 | 4600 | 0.412 |
| 79 | 4760 | 0.398 |
| 81 | 4880 | 3.208 |
| 85 | 5120 | 3.144 |
| 91 | 5480 | 0.396 |
| THD | | 4.56 |

It is shown from Table 5 that two harmonic components of 4.88 kHz and 5.12 kHz are dominant so, these components are considered in design of the transformer supplied by the converter. The total losses of the subjected transformer are calculated and given in Table 6.

**Table 6.** Total losses calculated according IEC method

| | $LV_1$ | HV | $LV_2$ |
|---|---|---|---|
| $I_{LN}$ (A) | 2233 | 85.44 | 2233 |
| $R_W$ (mΩ) | 0.42 | 2640 | 0.83 |
| $R_C$ (mΩ) | 0.12 | 150 | 0.11 |
| $P_{WE1}$ (W) | 82.5 | 534.6 | 164.5 |
| $F_{WE}$ | 8.56 | 4.16 | 8.83 |
| $P_{WEAX1}$ (W) | 43.66 | 180.9 | 84.98 |
| $P_{WERAD1}$ (W) | 35.71 | 361.81 | 146.51 |
| $F_{CE}$ | 1.07 | | |
| $P_{CE1} + P_{SE1}$ (W) | 3801.47 | | |
| $P_{Total\ Load\ Loss}$ (W) | 51031 | | |

From Table 6, it is seen that the total load losses of the PV transformer are calculated as 51 kW, which means that the total load loss increases by approximately 4.8 kW due to the presence of current harmonics.

### *2.7. Calculation of the Short Circuit Impedance*

The short-circuit impedance of the transformer consists of the resistive and reactive component realized using the following equation.

$$U_K = \sqrt{U_X^2 + U_R^2} \tag{12}$$

where $U_X$ and $U_R$ represent the resistive and reactive components respectively and can be calculated using the following equation [17];

$$U_X = 8\pi^2 \times \frac{I_{PH} \times f \times N^2 \times k \times \Delta \times 10^{-8}}{V_{PH}} \tag{13}$$

$$U_R = \frac{Load \cdot Loss}{S \times 10} \tag{14}$$

where f is the frequency, N is number of turns, K is rogowski factor, $I_{PH}$ and $V_{PH}$ are the phase current and phase voltage, respectively. The calculated impedances are given in Table 7.

**Table 7.** Short circuit impedance values

| | $LV_1$-HV | $LV_2$-HV |
|---|---|---|
| $\%U_X$ | 6.63 | 7.32 |
| $\%U_R$ | 0.54 | 0.76 |
| $\%U_K$ | 6.65 | 7.36 |

### *2.8. Calculation of The No Load Loss*

Core losses or no-load losses at rated frequency and voltage can be calculated using the following equation [17],

Core loss = Core weight × w/kg × building factor (15)

The core loss of the transformer is calculated as 3688 W, where the specific loss of the core material at 1.65 T is 0.98 W/kg and building factor is 1.26 for related step lap construction.

### 2.9. *Calculation of Thermal Ability to Withstand Short Circuit Current*

The maximum allowable value of the highest average temperature of the winding after 2 seconds of symmetrical short-circuit current is calculated using equation (16) to show whether the windings have the thermal ability to withstand the symmetrical short-circuit current [19].

$$\theta = \theta_0 + \frac{2\times(\theta_0 + 225)}{\left(\frac{45700}{J^2 \times t} - 1\right)} \quad (16)$$

where $\theta_0$ is the initial winding temperature and is assumed to be the sum of the maximum allowable ambient temperature and the temperature rise of the winding at nominal conditions. The calculated short-circuit temperatures of the windings are within the limits of 200°C for the Aluminum winding.

### 2.10. *Calculation of Tank Dimension of the Transformer*

The tank dimension of the transformer is carried out using the flowing steps;

- Tank length= 3 × LV2 winding outer diameter + 2 × phase to phase clearance + 2 × winding to tank short side clearance
- Tank width= LV2 winding outer diameter + Clearance to tank on HV side + Clearance to tank on LV side
- Tank height = Core window height + 2 × Maximum step width of core + Distance from the core surface to the tank cover

### 2.11. *Calculation of Top Oil Temperature Rise*

The cooling area (surface area) of the transformer is calculated to keep the top oil temperature rises of the transformer below 60˚C.

## 3. Simulation Result

The simulation is performed with a sinusoidal waveform using parameters obtained from the design such as the number of turns, core and coil design details. According to the simulation study, the primary and secondary winding current and voltage are calculated. The maximum current peak values for LV1, LV2 and HV windings are 3.04 kA, 3.11 kA and 117.6 A, respectively. The maximum voltage values for LV1, LV2 and HV windings are 0.931 kV, 0.929 kV and 48.49 kV, respectively.

Figure 2 shows no load losses of studied transformer with hysteresis and eddy losses obtained from the simulation result.

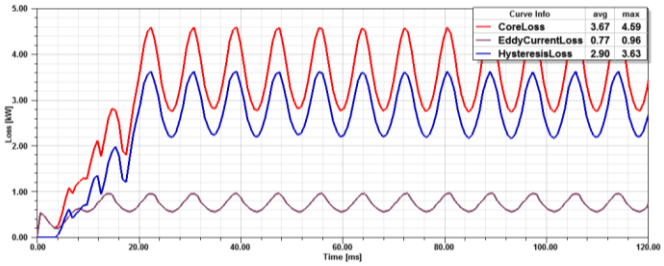


**Fig. 2.** PV transformer no load losses

To investigate the behavior of the transformer under distorted current, the simulation is performed in the presence of two dominant high-frequency current harmonic contents. Based on the results of this simulation, the maximum current peak values for $LV_1$, $LV_2$ and HV windings are 3.46 kA, 3.66 kA and 135.5 A, respectively. The maximum voltage values for $LV_1$, $LV_2$ and HV windings are 1.181 kV, 1.179 kV and 54.81 kV, respectively.

## 4. Experimental Measurements

Experimental tests were carried out on the transformer for sinusoidal input voltage due to the absence of PWM-based operating inverters. Experimental results were compared with those obtained from 3D FEM under the same conditions. General definitions and terms related to the requirements for routine tests of transformer and test circuits are given in [14].

The experimental setup used to measure the load and no-load losses and the short-circuit impedance is shown in Figure 3.

**Fig. 3.** The experimental setup used to measure losses and short circuit impedance

The results obtained from the simulation study and experiments are given in Table 8. In the simulation study, the winding eddy current loss is neglected since the winding is defined as a helical model and the simulation only runs with the active part of the transformer, and the connection losses and the losses of tank and core clamps of the transformer are also neglected.

## 4. Conclusion

In this paper, the design process of a 3-phase special type transformer fed by two separate inverters has been carried out. The results from the design procedure are compared with the results obtained from 3D FEM under the same conditions provided by the sinusoidal voltage. Comparison of the corresponding results given in Table 8 shows that the error is within an acceptable range. The harmonic content of the input voltage and current causes the transformer's power losses to increase, resulting in an increase in the operating temperature, which shortens the expected life of the transformer.

Experimental results obtained by applying a sinusoidal voltage were also compared with results obtained from 3D FEM for the same conditions. As shown in Table 8, the corresponding average error is low and is about 2.5%.

Though the results in general are in a good agreement, the errors related to the load losses are relatively high and this is due to the fact that the losses in the winding connections and the transformer tank have not been taken into account in the simulation studies.

The calculations and analyses carried on in this study verify the accuracy of the method used for the electrical design of the PV transformer to match the target performance and ensure the reliability of safe operation for the transformer subjected to certain operating conditions in solar power plants.

The approach used in this work to design a transformer for non-sinusoidal input voltage has a significant advantage over the so-called K-factor method used in the design of transformers for non-sinusoidal input voltage. Although the K-factor method can also be used in transformer design, the designed transformer will be large and uneconomical.

**Table 8.** Analysis results

| | | Sinusoidal current | | | Non-sinusoidal current | | |
|---|---|---|---|---|---|---|---|
| | | FEM | Test | Error (%) | FEM | Design | Error (%) |
| HV (V) | | 34285 | 34497 | -0.6 | 34476 | 34500 | -0.1 |
| $LV_1$ (V) | | 658 | 658.7 | -0.1 | 670 | 660 | 1.5 |
| $LV_2$ (V) | | 657 | 658.9 | -0.3 | 667 | | 1.1 |
| HV (A) | | 82.8 | 84.8 | -2.4 | 83.3 | 85.3 | -2.3 |
| $LV_1$ (A) | | 2138 | 2216.3 | -3.5 | 2147 | 2230.6 | -3.7 |
| $LV_2$ (A) | | 2195 | | -1.0 | 2224 | | -0.3 |
| No load (W) | | 3670 | 3613 | 1.6 | 3715 | 3688 | 0.7 |
| Load Loss (W) | $LV_1$ | 7448 | 8025 | -7.2 | 7550 | 8784 | -14.0 |
| | HV | 19076 | 20194 | -5.5 | 19320 | 22587 | -14.5 |
| | $LV_2$ | 13651 | 14140 | -3.5 | 14051 | 15588 | -9.9 |

## Acknowledgements

The author would like to thank SEM Transformatör Inc. for providing high quality test equipment and design tools for this study.

## References

1. M. A. Taher, S. Kamel and Z. M. Ali, "K-Factor and transformer losses calculations under harmonics," 2016 Eighteenth International Middle East Power Systems Conference (MEPCON), 2016, pp. 753-758, doi: 10.1109/MEPCON.2016.7836978.
2. IEEE Standard C. 57-110-2018, recommended practice for establishing liquid-filled and dry-type power and distribution transformer capability when supplying non-sinusoidal load currents, The Institute of Electrical and Electronics Engineers, 2018.
3. B. A. Thango, J. A. Jordaan, A. F. Nnachi, "Effects of Current Harmonics on Maximum Loading Capability for Solar Power Plant Transformers" International SAUPEC/RobMech/PRASA Conference, 2020, pp. 1-5, doi:10.1109/SAUPEC/RobMech/PRASA48453.2020.9041101.
4. B. A. Thango, J. A. Jordaan, A. F. Nnachi, "Step-Up Transformers for PV Plants: Load Loss Estimation under

Harmonic Conditions," 2020 19th International Conference on Harmonics and Quality of Power (ICHQP), 2020, pp. 1-5, doi: 10.1109/ICHQP46026.2020.9177938.

5. S. Kül, B. Yildiz, B. Tamyurek and I. Iskender, "Coreloss Estimation via Long Short-Term Memory Model (LSTM) of Dry-Type Transformer based on FEA," 2021 10th International Conference on Renewable Energy Research and Application (ICRERA), 2021, pp. 357-361, doi: 10.1109/ICRERA52334.2021.9598631.

6. M. S. Chaouche, H. Houassine, S. Moulahoum and I. Colak, "Finite element method to construct a lumped parameter ladder network of the transformer winding," 2017 IEEE 6th International Conference on Renewable Energy Research and Applications (ICRERA), 2017, pp. 1092-1096, doi: 10.1109/ICRERA.2017.8191224.

7. I. R. Macías Ruiz, L. A. Trujillo Guajardo, L. H. Rodríguez Alfaro, F. Salinas Salinas, J. Rodríguez Maldonado, and M. A. González Vázquez, "Design Implication of a Distribution Transformer in Solar Power Plants Based on Its Harmonic Profile," Energies, vol. 14, no. 5, p. 1362, Mar. 2021, doi: 10.3390/en14051362. [Online]. Available: http://dx.doi.org/10.3390/en14051362

8. J. Yaghoobi, A. Alduraibi, D. Martin, F. Zare, D. Eghbal, R. Memisevic, "Impact of high-frequency harmonics (0–9 kHz) generated by grid-connected inverters on distribution transformers", International Journal of Electrical Power & Energy Systems, vol. 122, November 202. doi.org/10.1016/j.ijepes.2020.106177

9. IEC Standard 61378-1, Converter Transformers - Part 1: Transformers for Industrial Applications, International Electrotechnical Commission, 2011.

10. IEC Standard 61378-3, Converter Transformers - Part 3: Application Guide, International Electrotechnical Commission, 2015.

11. IEEE Standard C57.159-2016, Guide on Transformers for Application in Distributed Photovoltaic (DPV) Power Generation Systems, The Institute of Electrical and Electronics Engineers, 2016.

12. M. Cyril Hlatshwayo, "The Computation of Winding Eddy Losses in Power Transformers Using Analytical and Numerical Methods", University of the Witwatersrand, 2011.

13. K. Iyer, Transformer Winding Losses with Round Conductors and Foil Windings for Duty-Cycle Regulated Square Waveform Followed by Winding Design and Comparison for Sinusoidal Excitation, University of Minnesota, 2013.

14. IEC Standard 60076-1, Power transformers – Part 1: Part 1: General, International Electrotechnical Commission, 2011.

15. IEC Standard 60076-2, Power transformers – Part 2: Temperature rise for liquid-immersed transformers, International Electrotechnical Commission, 2011.

16. IEC Standard 60076-3, Power transformers – Part 3: Insulation levels, dielectric tests and external clearances in air, International Electrotechnical Commission, 2013.

17. K.R.M. Nair, Power and Distribution Transformers Practical Design Guide, CRC Press, 2021

18. IEC Standard 60076-7, Power transformers – Part 7: Loading guide for oil-immersed power transformers, International Electrotechnical Commission, 2013.

19. IEC Standard 60076-5, Power transformers – Part 5: Ability to withstand short circuit, International Electrotechnical Commission, 2006.

20. A.Shobole, M.Baysal, M.Wadi, M.Tur, "Effects of Distributed Generations' Integration to the Distribution Networks Case Study of Solar Power Plant", International Journal of Renewable Energy Research, vol. 7, no. 2, pp. 954-964, June. 2017.

21. D. Foito, V. F. Pires, A. Cordeiro and J. F. Silva, "Sliding Mode Vector Control of Grid-Connected PV Multilevel Systems Based on Triple Three-Phase Two-Level Inverters," 2020 9th International Conference on Renewable Energy Research and Application (ICRERA), 2020, pp. 399-404, doi: 10.1109/ICRERA49962.2020.9242782.

22. D. Gueye, A. Ndiaye and A. Diao, "Adaptive Controller Based on Neural Network Artificial to Improve Three-phase Inverter Connected to the Grid," 2020 9th International Conference on Renewable Energy Research and Application (ICRERA), 2020, pp. 72-77, doi: 10.1109/ICRERA49962.2020.9242740.

23. M. Khatri, A. Kumar, "Experimental Investigation of Harmonics in a Grid-Tied Solar Photovoltaic System", International Journal of Renewable Energy Research, vol. 7, no. 2, pp. 901-907, June. 2017.

24. V. Castiglia, R. Miceli, G. Schettino, F. Viola, C. Buccella, C. Cecati, M.C. Cimoroni, "Mixed Harmonic Elimination Control for a Single-Phase 9 Level Grid-Connected Inverter," 2018 International Conference on Smart Grid (icSmartGrid), 2018, pp. 240-245, doi: 10.1109/ISGWCP.2018.8634487.

25. A. Jahi, I. Iskender, "Performance Analyses of a Three Winding Double Stack PV Transformer" International Journal on Technical and Physical Problems of Engineering, vol.13,no. 4, 20-25, December. 2021.